MATHEMATICAL MODELING OF SILICON SINGLE CRYSTAL INDUSTRIAL GROWTH

Dr. Andris Muižnieks, Dr. Andis Rudevičs, Dr. Armands Krauze, BSc. Vadims Suškovs, BSc. Kirils Surovovs, BSc. Kārlis Janisels

1. Introduction

The acticity was led by associated professor, Dr.-Phys. Andris Muiznieks. In the activity participated Dr.-Phys. Armands Krauze, Dr.-Chem. Girts Barinovs and several students of bachelor program in Physics.

In the frame of activity for the mathematical modeling of silicon single crystal growth by floating zone (FZ) method previously developed system of mathematical models and program package FZone were developed further. The integrated model of the argon flow in the FZ equipment was implemented in package FZone which allows for the first time to consider the interaction between the temperature distribution in the silicon and argon flow. For the first time the threedimensional (3D) mathematical model for the calculation of the molten zone shape and the temperature field inside it was developed and implemented in the package FZone. The package FZSiFOAM for the 3D calculation of temperature, hydrodynamic and dopant concentration field in the molten zone was developed further. This package is based on the open source code library OpenFOAM and is implemented on multiprocessor cluster in LINUX environment.
The description of the actual model system and program package FZone is given in the following sections.

2. Summary of actual mathematical model for FZ silicon single crystal growth

The actual calculation scheme of the program complex *FZone* is shown in Fig. 2.1. The temperature field in the silicon parts and temperature and velocity fields in the argon atmosphere is calculated as axis-symmetric. The high frequency (HF) electromagnetic (EM) field is calculated in three dimensions (3D). Melt free surface can be modeled as axis-symmetric or in three dimensions because the distribution of the electromagnetic pressure produced by a high-frequency inductor can be strongly non-symmetric. The flow, temperature and dopant transport in the molten zone is calculated in 3D. The calculated three-dimensional temperature field in melt is azimuthally averaged and used in *FZone* for phase boundary calculations.

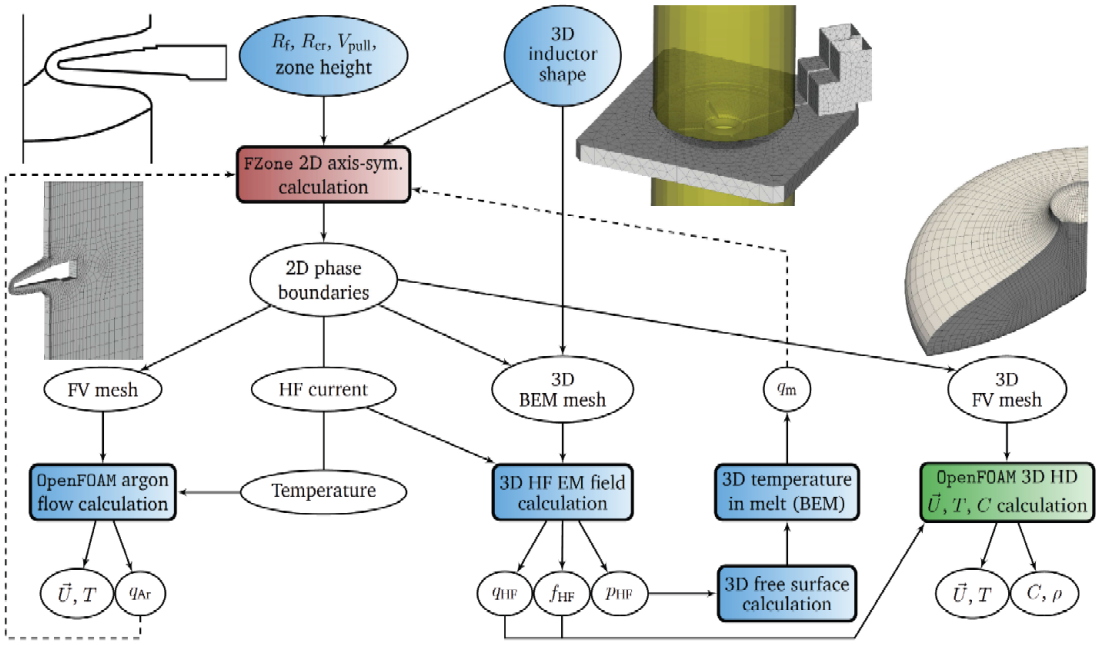

Fig. 2.1. The actual calculation scheme of the program complex *FZone*

In the case of neglecting convective heat transport in the molten zoneand the influence of argon flow, a simpler scheme can be used, in which only HF EM field is considered in 3D or in 2D, see Fig.2.2. Fig.2.2 also shows a corresponding axis-symmetric calculation example. Shown is the finite element mesh in the feed rod (polycrystal) and in the single crystal, temperature field in the melt and magnetic field lines produced by a high-frequency inductor. Fig. 2.3. shows the alculated three-dimensional distribution of electromagnetic power density induced by a high-frequency inductor on the free melt and crystal surfaces.

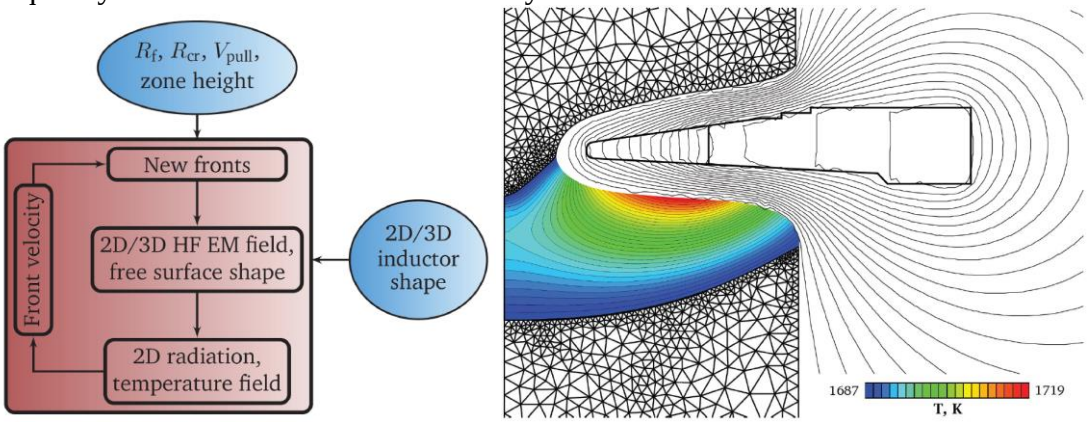

Fig. 2.2. A simpler calculation scheme, in which only HF EM field is considered in 3D or in 2D (left) and an axis-symmetric calculation example

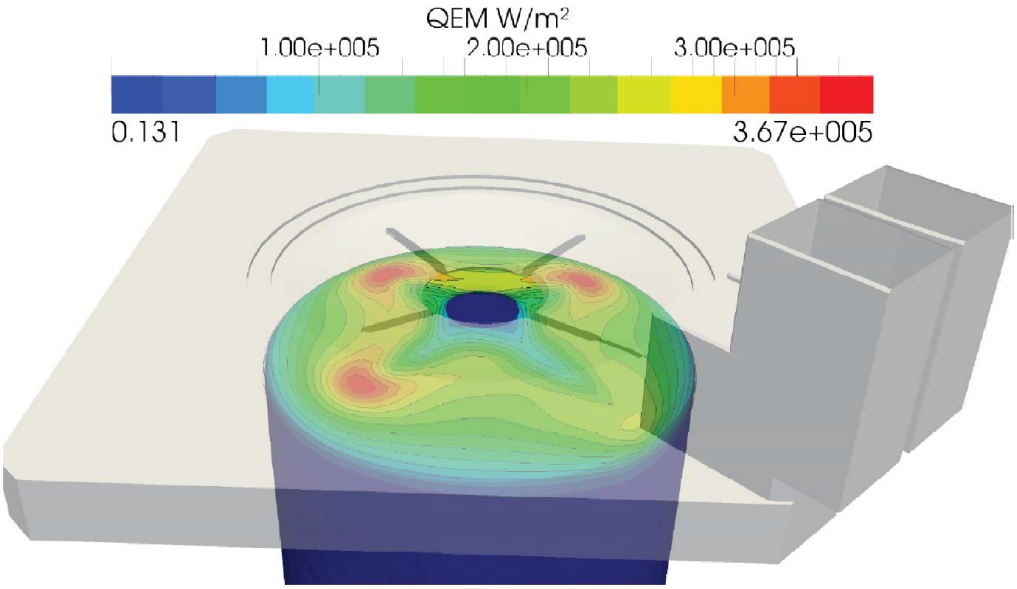

Fig. 2.3. Three-dimensional distribution of electromagnetic power density induced by a high-frequency inductor on the free melt and crystal surfaces

3. Three-dimensional model for asymmetric free surface influence on the FZ growth

To obtain a steady state three-dimensional (3D) solution for the FZ zone process, the following iterative model was developed, see Fig. 3.1. A special program module in (*FZone*) carries out high frequency EM field 3D calculations for a given inductor current. The result is the distribution of the EM pressure on the free surface. Another program recalculates the form of the free surface, which is influenced by EM pressure. To obtain a steady-state form of the free surface, the EM and free surface calculations are repeated iteratively until precision condition is satisfied. After that, a 3D boundary element calculation is run for the temperature distribution in the melt. It uses the EM heat distribution on the free surface as a part of the absorbed heat. The calculation results from the 3D BEM program are supplied to a 2D heat transfer program that models the heat transfer in the whole FZ system and updates the geometry of it. The procedure is repeated until a solution is found.

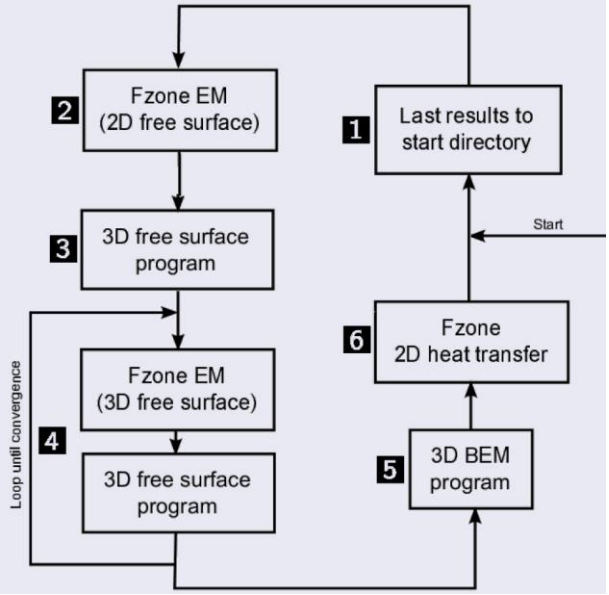

Fig. 3.1. General iterative scheme for the 3D calculation of the shape of the molten zone, 3D calculation of the temperature in the molten zone and coupling with FZone

For modeling the 3D free surface shapes, the method is used, which corresponds to the method used in licence free program ”Surface Evolver”. This method was improved by adding the EM pressure influence on the melt shape. For the 3D calculation of the temperature field in the molten zone, the 3D boundary element method is used with following boundary conditions: the temperature on the melting and crystallization interfaces is set constant; on the melt free surface the heat flux density is set, which is obtained from EM heat sources in the skinlayer and takes into account the heat radiation.

A calculation example is shown in Fig. 3.2and Fig. 3.3. The calculated system corresponds to one experimental setup for FZ 4” silicon crystal growth in the Institute for Crystal Growth in Berlin.

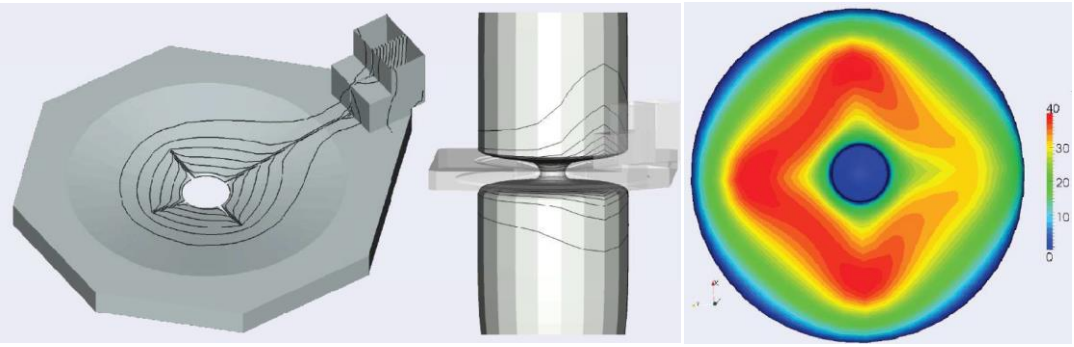

Fig. 3.2. HF inductor with the main slit and additional slits, 3D alculated surface current lines distribution (left); 3D calculated temperature distribution on the melt free surface (right)

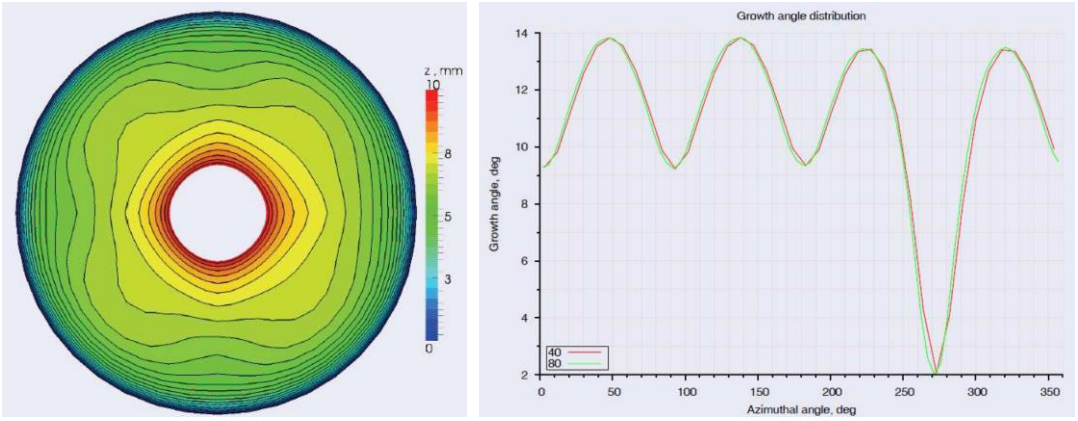

Fig. 3.3. Left: calculated 3D shape of the melt free surface (isolines of free surface z coordinate), the influence of additional slits and of main slits can be seen. Right: azimuthal distribution of the angle between the melt free surface and vertical direction at the triple point line

4. Modeling of argon flow heat transfer influence in FZ silicon single crystal growth

In practical FZ silicon single crystal growth systems, the argon atmosphere is always present (with pressure of some bar). Because this atmosphere can influence the heat exchange in the system, an axis-symmetric two-dimensional mathematical model for turbulent argon flow and heat transfer in FZ system was developed and implemented as program based on the open code library OpenFOAM.

4.1. Mathematical model of argon atmosphere

Argon is modeled as an ideal gas, therefore its density is

$$\rho = p\frac{M}{RT}$$

where p is the pressure, M is the molar mass of argon, R = 8.314 J/(K·mol) is the universal gas constant, T is the absolute temperature. In calculations the following values $p_0 = 2 \cdot 10^5$ Pa (reference pressure), M = 40 g/mol and c_p = 520 J/(kg·K) were used.

In a practical FZ puller, the density due to temperature differences in the system varies 3-4 times, therefore the argon flow is buoyancy-driven. The steady state of this compressible-like flow is described by continuity equation

$$\nabla\left(\rho\mathbf{U}\right) = 0$$

and Navier-Stokes equations

$$\nabla\left(\rho\mathbf{U}\mathbf{U}\right) = -\nabla\left(p_{\text{rgh}} + \frac{2}{3}\mu_{\text{eff}}\nabla\mathbf{U}\right) - \mathbf{g}\,\mathbf{x}\,\nabla\rho + \\ + \nabla\left[\mu_{\text{eff}}\left(\nabla\mathbf{U} + \nabla\mathbf{U}^T\right)\right],$$

where U is the velocity, $p_{rgh} = p - \rho g\, x$, $\mu_{eff} = \mu + \mu_t$ is the effective dynamic viscosity of argon (μ – molecular, μ_t – turbulent, obtained from turbulence model), g = 9.81 m/s^2 is standard gravity, x is spatial position vector. Turbulence is modeled using the SST k-omega low-Re turbulence model. The dependence of molecular dynamic viscosity on temperature $\mu(T)$ is given by Sutherland's law (Fig. 4.1).

$$\mu(T) = \frac{A_S\sqrt{T}}{1 + T_S/T}$$

Energy transfer in the FZ system is calculated using the enthalpy formulation

$$\rho \mathbf{U} \nabla h - \nabla\left(\alpha_{\text{eff}} \nabla h\right) = \mathbf{U} \nabla p,$$

where h is the enthalpy and $\alpha_{eff} = \alpha + \alpha_t$ is the effective thermal diffusivity for enthalpy (α – molecular, α_t – turbulent). Constant specific heat capacity at constant pressure c_p is assumed, therefore $h = c_p T$.

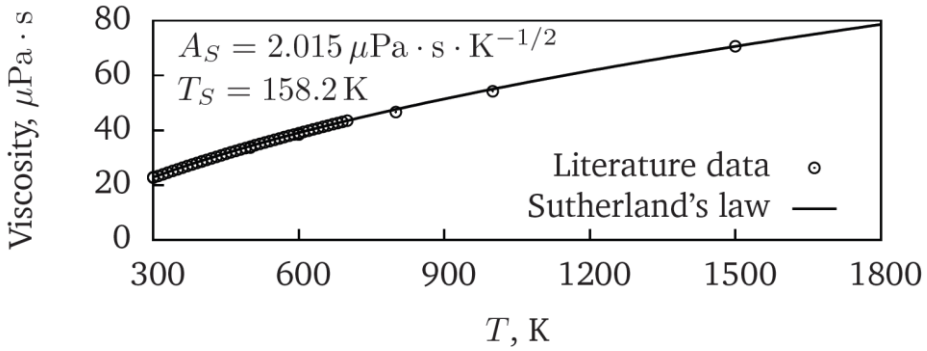

Fig. 4.1. The dependence of molecular dynamic viscosity on temperature $\mu(T)$ by Sutherland's law.

For the velocity field and enthalpy field the following boundary conditions (BC) are used: 1) Velocity: no-slip BC at solid walls (Si, inductor and puller wall surfaces); crystal pulling and rotation is neglected; 2) Temperature: first-type BC at solid walls; 3) Turbulent quantities: standard low-Re model BC at solid walls; 4) Axial symmetry: *wedge* BC at front and back planes.

4.2. Calculation algorithm

Because the temperature field in the argon and the temperature field in silicon parts and in the inductor are coupled, the following calculation algorithm was developed (see Fig. 4.2):

1) Calculation of the quasi-stationary shape of phase boundaries with the program *FZone*;
2) Creation of the geometry for argon flow calculations and mesh generation;
3) Interpolation of the temperature field on the Si surfaces from *FZone* to the generated mesh boundary;
4) Calculation of the axisymmetric steady state argon flow using *OpenFOAM* standard solver *buoyantSimpleFoam*;

5) Calculation of the quasi-stationary shape of phase boundaries using *FZone* with argon heat flux density (obtained in the previous step using utility *wallHeatFlux*) taken into account.

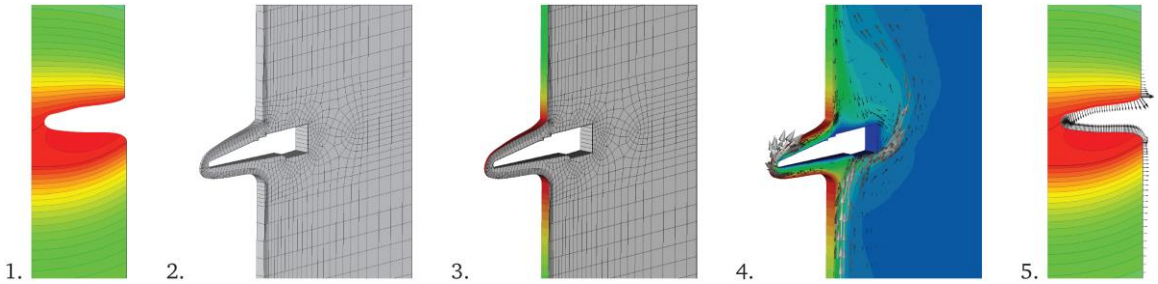

Fig. 4.2. Calculation steps in the used algorithm for the coupling of the temperature fields in argon atmosphere and in silicon parts and in the inductor

4.3. Calculation example

A typical ICG (Berlin) FZ system with crystal diameter 4" and mono- and polycrystal lengths 1 m has been considered. FZ puller height is 3 m, radius – 30 cm, the generated finite element mesh consists of ca. 50,000 cells.

The results of calculation are given in the following figures: in Fig. 4.3 the temperature and velocity fields in the vicinity of the inductor are shown; in Fig. 4.4 detailed views of temperature and velocity fields at crystal surface, velocity magnitude, stream function isolines and viscosity ratio μ_t/μ are given; in Fig. 4.5 the influence of additional crystal cooling by argon on the quasi-stationary shape of phase boundaries is shown.

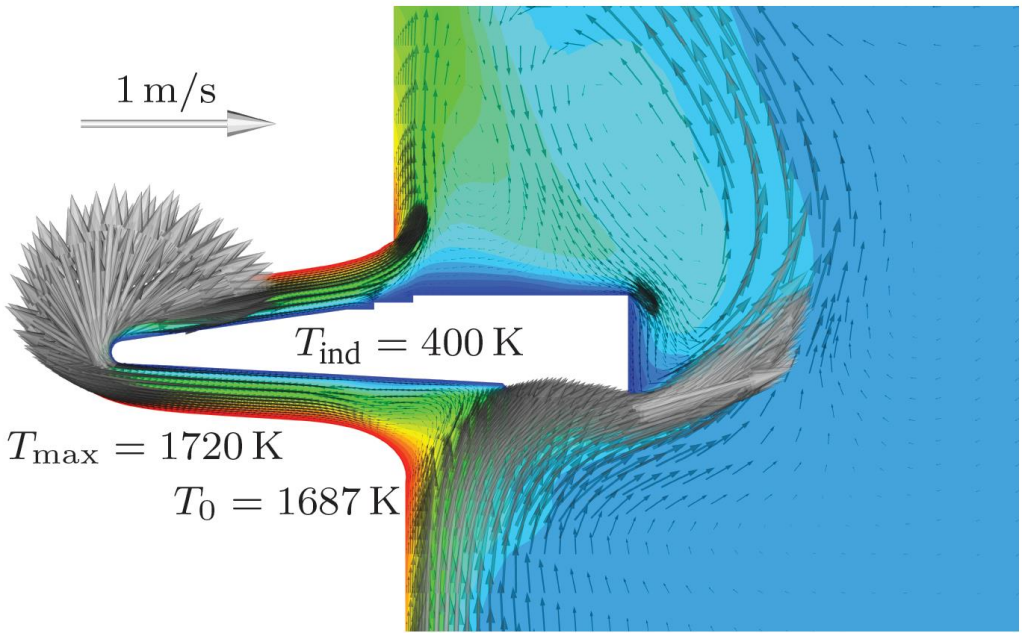

Fig. 4.3. Calculated temperature and velocity fields in the vicinity of the HF inductor.

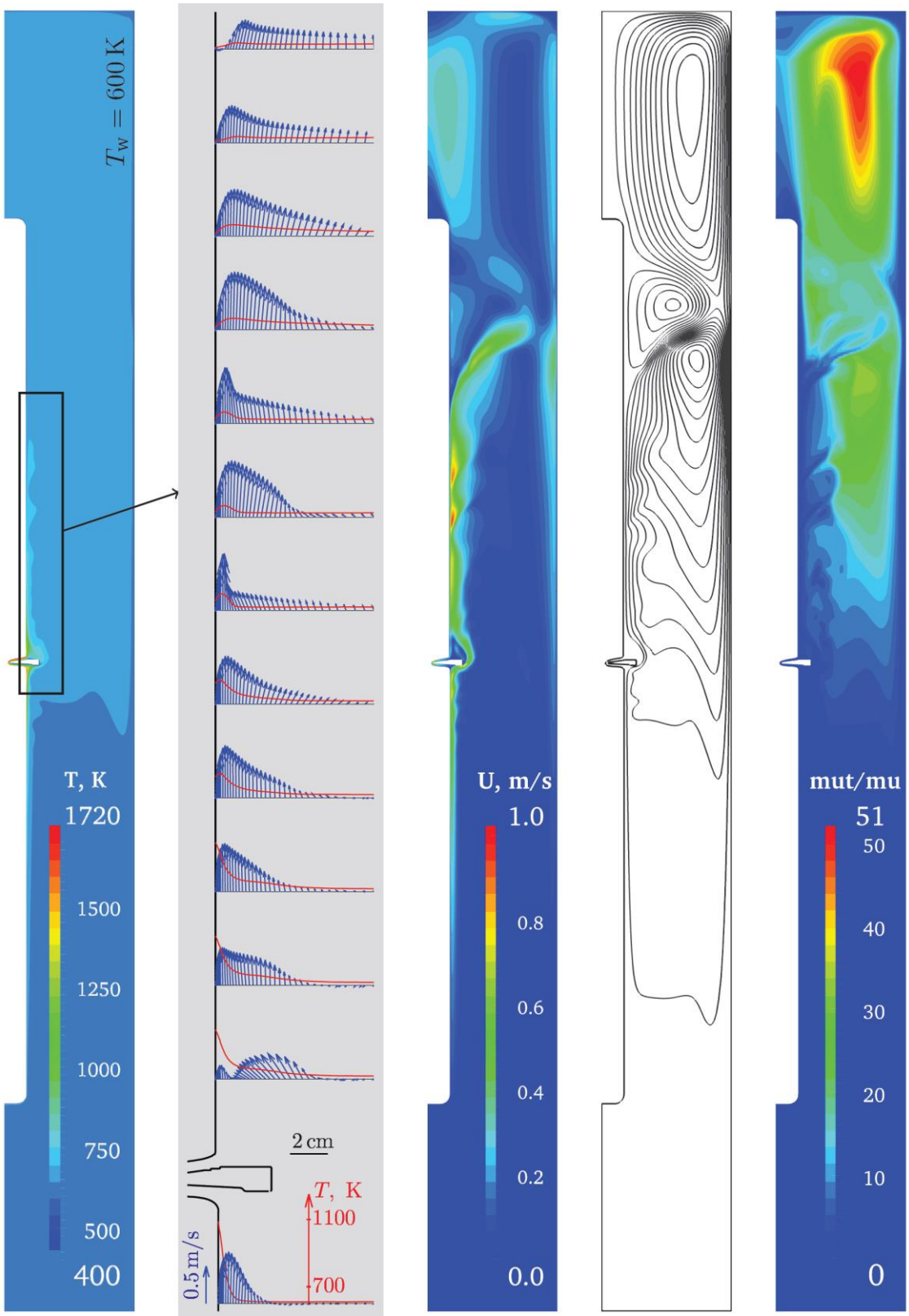

Fig. 4.5. From left to right: temperature, detailed views of temperature and velocity fields at crystal surfaces, velocity magnitude, stream function isolines, viscosity ratio μ_t/μ.

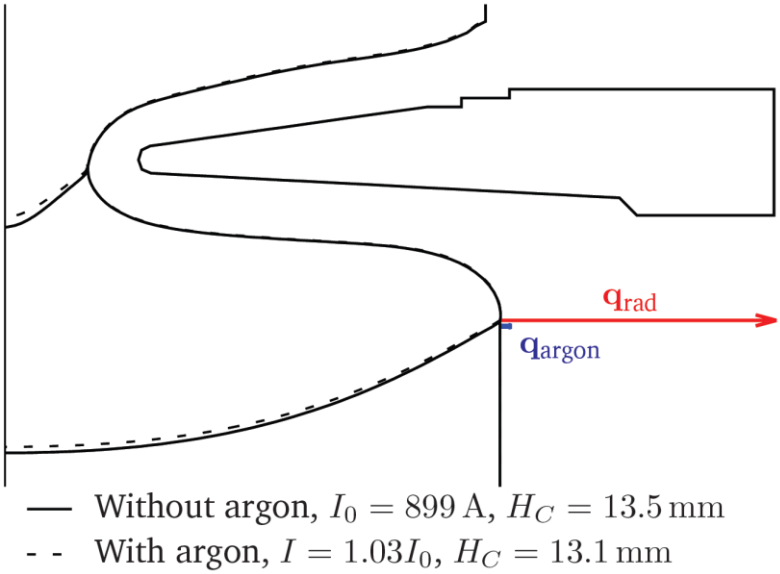

Fig. 4.5. The influence of additional crystal cooling by argon on the quasi-stationary shape of phase boundaries. I is inductor current, H_C is crystallization interface deflection.

5. Three dimensional (3D) modeling of melt motion using *FZSiFOAM*

For the 3D modeling of the melt flow in the molten zone, the previously self developed calculation program FZSiFOAM (which is based on the program library OpenFOAM) was further developed. New and more precise boundary conditions were implemented in the program for the dopant concentration field.

The calculated melt flow and concentration fields for a 4” silicon single crystal growth system at the Institute for Crystal Growth (Berlin) are presented in the following figures. Fig. 5.1 illustrates the preparation of the 3D geometry of silicon for HF EM calculations. Fig. 5.2 shows a calculation setup on a Linux cluster. In Fig. 5.3 a schematic example of computational domain subdivision into 4 parts is given; each part is solved separately on one processor. Fig. 5.4 shows calculated axis-symmetric shape of phase boundaries and temperature field in melt. A schematic view of a typical melt motion pattern in a FZ system is given in Fig. 5.5. In Fig. 5.6 a fragment of used 3D finite volume mesh for melt domain (left)and a closer look at the boundary layer at the crystallization interface (right) are shown. Fig. 5.7 shows the calculated time-averaged temperature field and velocity field on the melt free surface. The calculated time-averaged velocity field in the inductor main slit plane (top) and perpendicular to it (bottom) is given in Fig. 5.8. In Fig. 5.9 the calculated concentration field at the crystallization interface with instantaneous snapshot (left) and time-averaged field (right) is shown. Fig. 5.10 represents the calculated radial resistivity profiles.

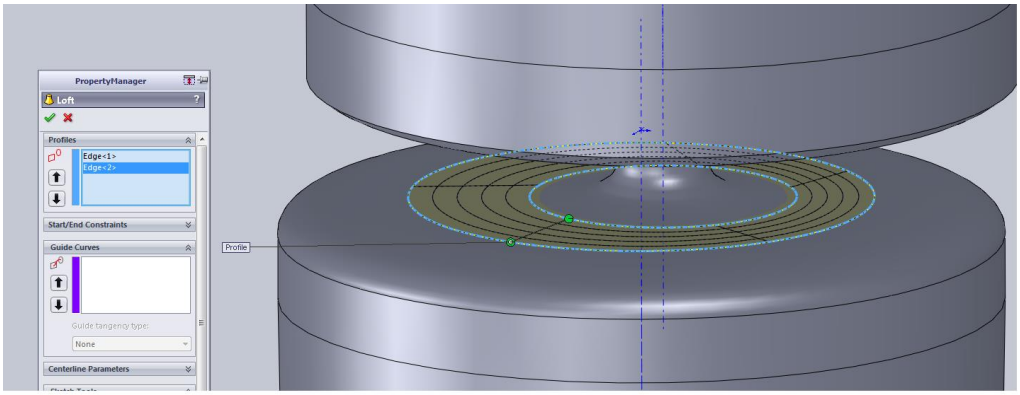

Fig. 5.1 The preparation of the 3D geometry of silicon for HF EM calculations.

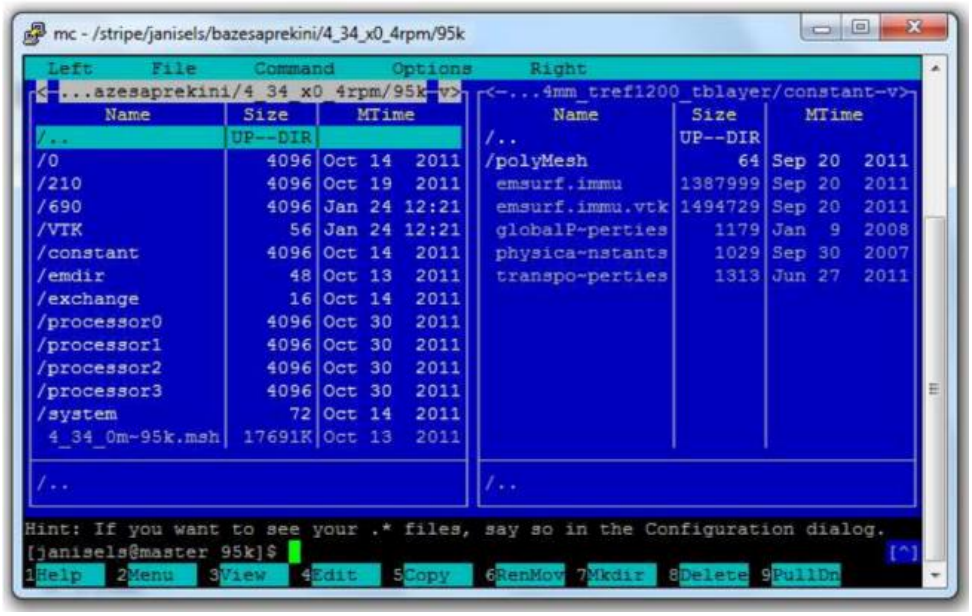

Fig. 5.2. Calculation setup on a Linux cluster.

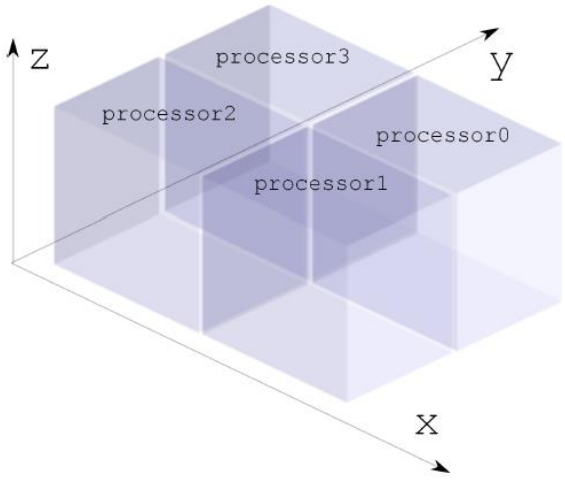

Fig. 5.3. A schematic example of computational domain subdivision into 4 parts; each part is solved separately on one processor.

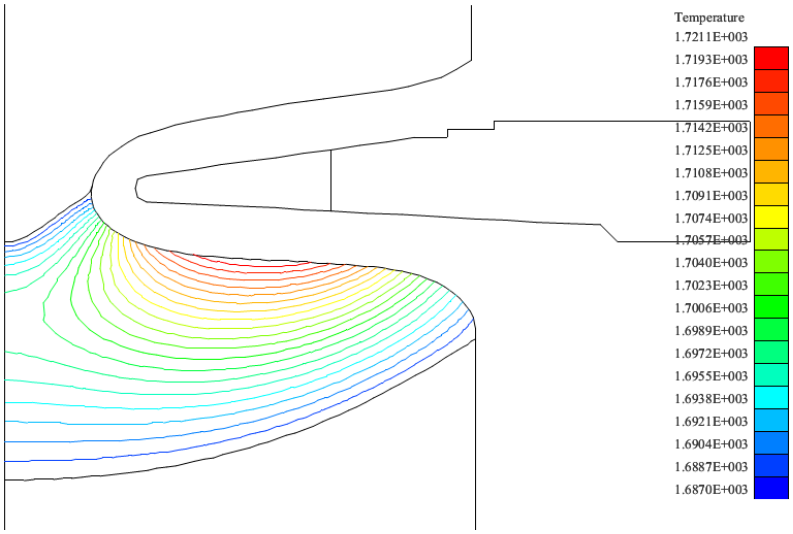

Fig. 5.4. Calculated axis-symmetric shape of phase boundaries and temperature field in melt.

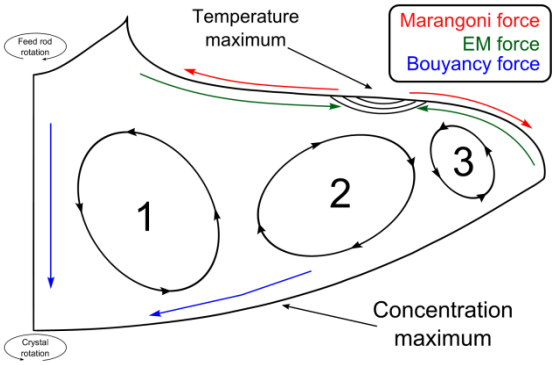

Fig. 5.5. A schematic view of a typical melt motion pattern in a FZ system.

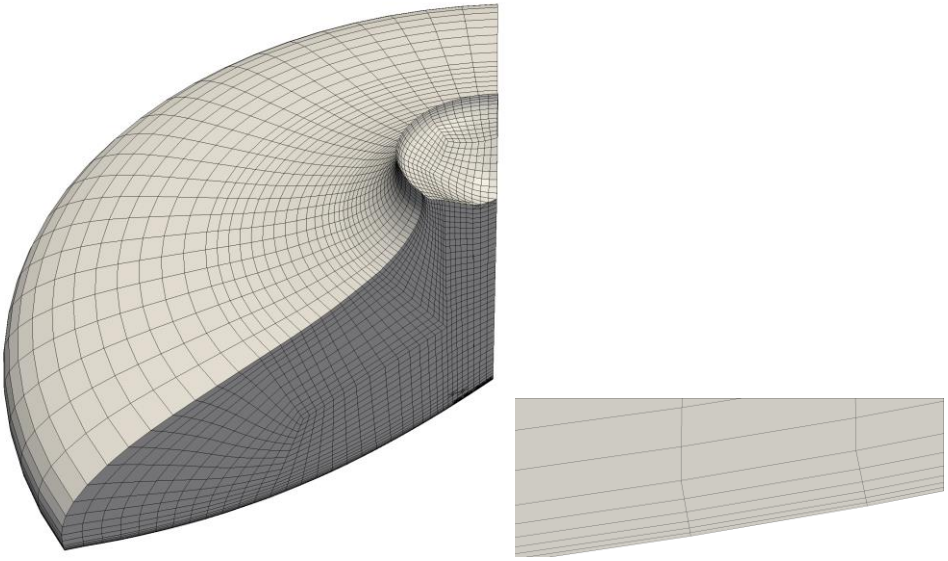

Fig. 5.6. Fragment of used 3D finite volume mesh for melt domain (left); a closer look at the boundary layer at the crystallization interface (right).

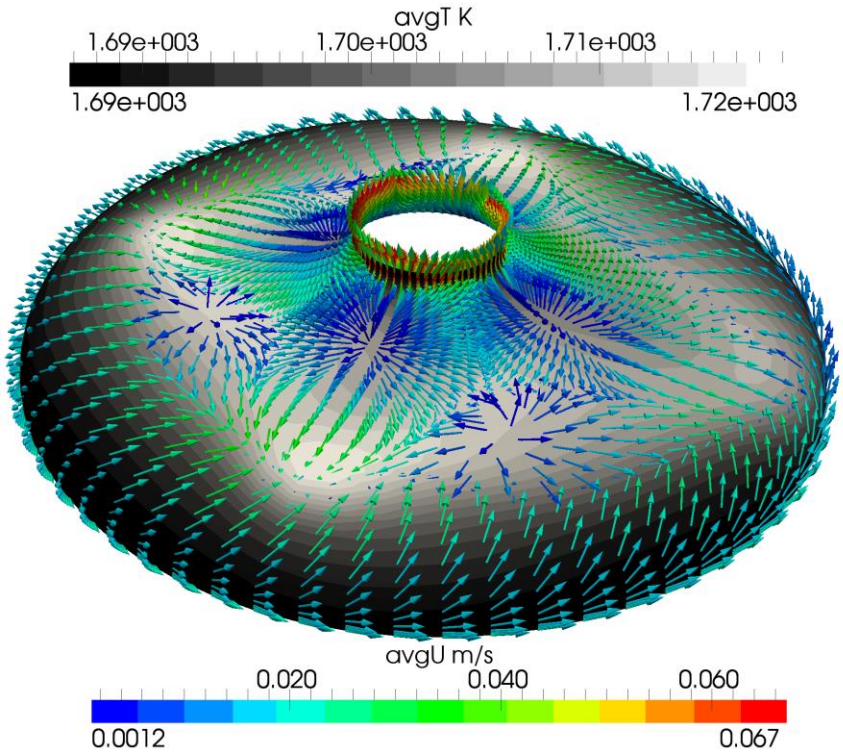

Fig. 5.7. The calculated time-averaged temperature field and velocity field on the melt free surface.

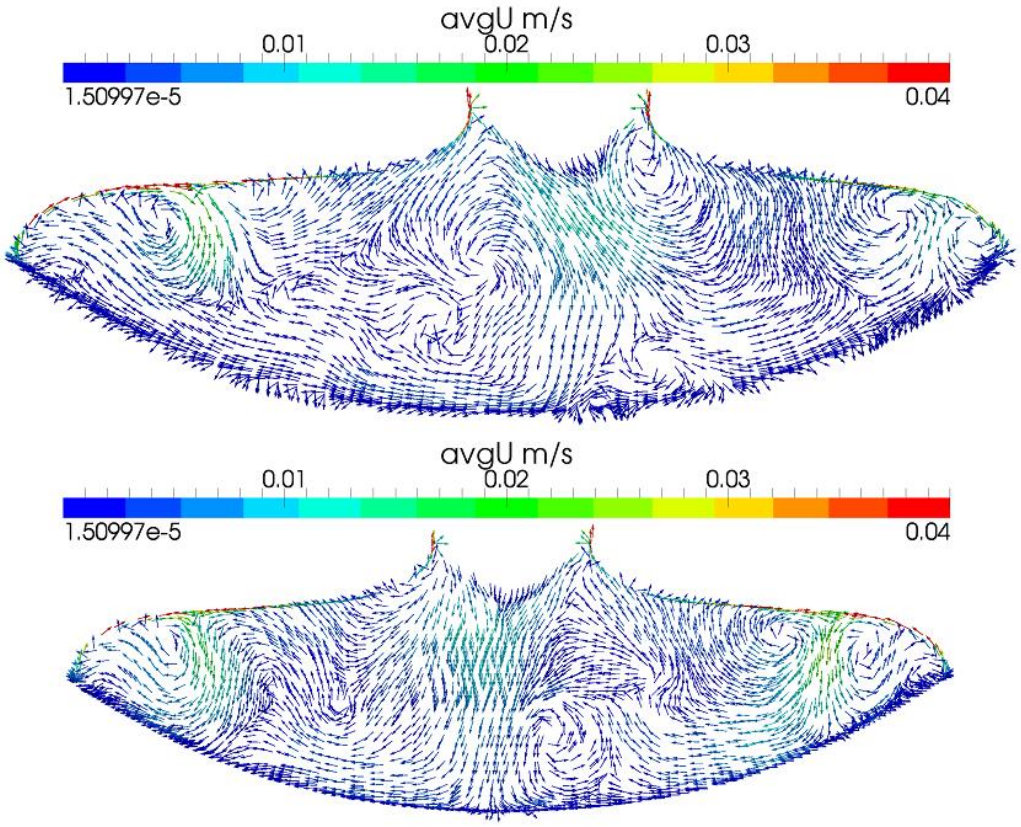

Fig. 5.8. The calculated time-averaged velocity field in the inductor main slit plane (top) and perpendicular to it (bottom).

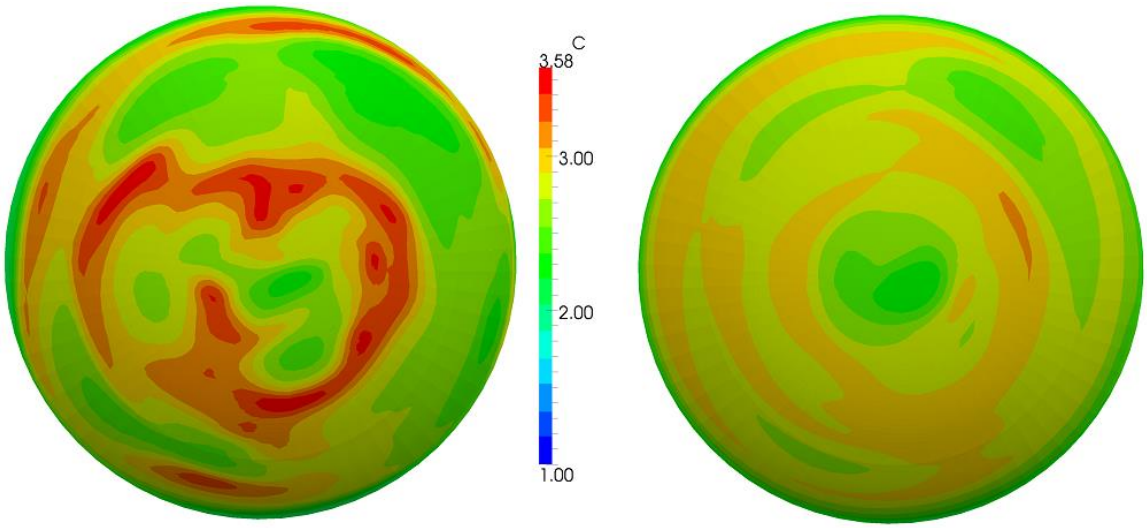

Fig. 5.9. The calculated concentration field at the crystallization interface; instantneous snapshot (left) and time-averaged field (right).

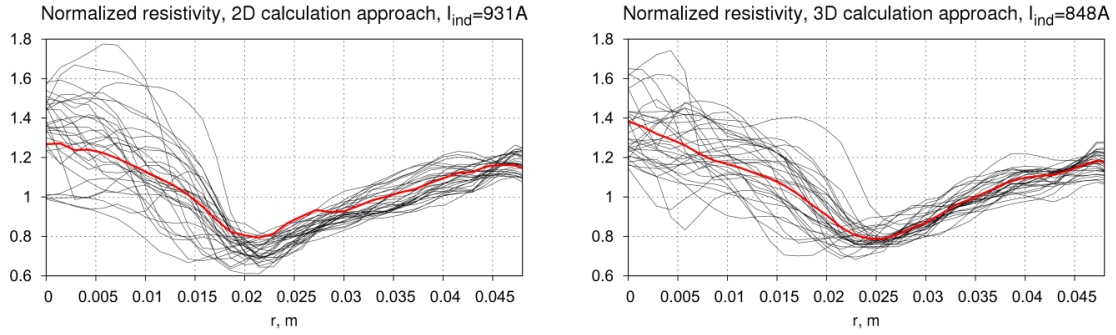

Fig. 5. 10. The calculated radial resistivity profiles in the grown crystal.

The results of activity were reported in the following international conferences as oral or poster presentations:

1. 5th International Workshop on Crystal Growth Technology, Berlin, Germany, June 26-30, 2010.
2. 6th International Scientific Colloquium "Modelling for Material Processing", Riga, September 16-17, 2010.
3. *"Deutsche Kristallzüchtungstagung 2012",* Freiberg, Germany, March 7-9, 2012.
4. *"4th European Conference on Crystal Growth",* Glasgow, Scotland, June 17-21, 2012.
5. "8.Workshop – Angewandte Simulation in der Kristallzuechtung", Potsdam, Germany, November 19-21, 2012.
6. Functional Materials and Nanotechnologies, Riga, April 2012.

Publications

1. **A. Krauze, A. Muiznieks, K. Bergfelds, K. Janisels, G. Chikvaidze**. Reduction of silicon crust on the crucible walls in silicon melt purifying processes with electron beam technology by means of low-frequency traveling magnetic fields. Magnetohydrodynamics, 2011, Vol. 47, No. 4, 369-383.
2. **A. Muiznieks, K. Lacis, A. Rudevics, U. Lacis, A. Sabanskis, M. Plate**. Development of numerical calculation of electromagnetic fields in FZ silicon crystal growth process. Magnetohydrodynamics, 2010, Vol. 46, No. 4, 475-486.
3. **K. Lacis, A. Muiznieks, A. Rudevics, A. Sabanskis**. Influence of DC and AC magnetic fields on melt motion in FZ large Si crystal growth. Magnetohydrodynamics, 2010, Vol. 46, No. 2, 199-218.
4. **A. Krauze, N. Jekabsons, A. Muiznieks, A. Sabanskis, U. Lacis**. Applicability of LES turbulence modeling for CZ silicon crystal growth systems with traveling magnetic field. Journal of Crystal Growth, 2010, Volume 312, Issue 21, 3225-3234.